ELSEVIER

Physica C 371 (2002) 97–103

PHYSICA C

www.elsevier.com/locate/physc

Deposition and interface structures of YBCO thin films via a non-fluorine sol–gel route

Donglu Shi [a,*], Yongli Xu [a], S.X. Wang [b], J. Lian [b], L.M. Wang [b], Shaun M. McClellan [a], Relva Buchanan [a], K.C. Goretta [c]

[a] *Department of Materials Science and Engineering, University of Cincinnati, 497 Rhodes Hall, Cincinnati, OH 45221-0012, USA*
[b] *Department of Nuclear Engineering and Radiological Science, University of Michigan, Ann Arbor, MI 48109, USA*
[c] *Energy Technology Division, Argonne National Laboratory, Argonne, IL 60439-4838, USA*

Received 8 June 2001; received in revised form 20 August 2001; accepted 23 August 2001

Abstract

Previous work on $YBa_2Cu_3O_x$ (YBCO) thin films deposited by fluorine-based sol–gel synthesis has been extensively reported. To further develop grain-textured YBCO thin films for conductor development, we deposited, via a fluorine-free sol–gel synthesis, YBCO thin films on single crystal substrates of yttrium-stabilized zirconia (YSZ) and $LaAlO_3$ (LAO). Sol–gel-derived films on the YSZ and LAO substrates exhibited epitaxial growth. This result was confirmed by both X-ray diffraction (XRD) and high-resolution transmission electron microscopy (HRTEM). A transport J_c above 10^5 A/cm^2 has been reached at 77 K and zero magnetic field. Experimental details are reported on the sol–gel synthesis, XRD and HRTEM characterization of the YBCO thin films. Also discussed is the underlying crystallization mechanism of the YBCO phase on these substrates.

Keywords: YBCO; Coated conductor; Sol–gel; Texturing; Interfaces; Thin film

1. Introduction

In large-scale applications of superconductors, the conductors are required not only to carry high critical current density at respectable magnetic fields, but also to possess high ductility, mechanical strength, and stability. To improve the transport properties of high-temperature superconductors, extensive experimental investigations have been carried out in developing highly textured thin films on a variety of substrates [1–5]. The fabrication of $YBa_2Cu_3O_x$ (YBCO) films by epitaxial deposition on rolling assisted biaxially textured substrates (RABiTS) has proved to be successful in the conductor development for large-scale applications [1,2]. The RABiTS technique uses well-established, industrially scaleable, thermomechanical processes to impart a high degree of grain texture to a base metal. Buffer layers are then deposited to yield chemically and structurally compatible surfaces. Epitaxial YBCO films are grown on such a surface, resulting in a critical current density at 77 K on the order of 10^6 A/cm^2 [1,2]. This approach has shown a promise for

* Corresponding author. Tel.: +1-513-556-3100; fax: +1-513-556-1004.
E-mail address: dshi@uceng.uc.edu (D. Shi).

0921-4534/01/$ - see front matter
PII: S0921-4534(01)01075-9

developing long conductors for industrial applications.

In our previous work [4,5], we have shown the possibilities of obtaining *c*-axis grain orientated YBCO thick films on silver alloy substrates via high-temperature melt processing. Such a thick-film approach may serve as an alternative to the vapor deposition methods. The advantages of this approach includes: (1) YBCO is in direct contact with the metallic substrate that serves as a stablizer; (2) it can be readily scaled up into long-length conductors; (3) the large cross-sectional area of the thick film can potentially carry high engineering J_cs; (4) no buffer layer is needed, so that the processing is straightforward and simple; and (5) the cost is much less than for the vapor deposition methods.

Based on the knowledge and experimental data from the deposition of YBCO thick films on metallic substrates, we attempted to develop another viable approach to fabricating coated conductors. We selected a non-fluorine, sol–gel method because of the difficulties with HF evolution from F-containing systems [6–15]. To study the sol–gel chemistry of YBCO, in this work, we deposited the YBCO films on single-crystal substrates of yttrium-stablized zirconia (YSZ) and $LaAlO_3$ (LAO). In this study, we present the experimental results of sol–gel synthesis and characterization of the YBCO thin films.

2. Experimental

There have been extensive reports on fluorine-based sol–gel process for the deposition of YBCO films [6–14]. Our non-fluorine-based sol–gel YBCO solutions were developed in-house. For the precursor solution, stoichiometric (1:2:3) yttrium trimethyl acetate, barium hydroxide, and copper trimethyl acetate powders (ALDRICH, 99.99%) were dissolved in a mixture of propionic acid/amine solvent with an oxide concentration between 0.1 and 0.5 mol/l. The addition of amine was important because it greatly improved the solubility of the precursor powders in propionic acid. The stock solution was stable in air with a shelf life longer than two years. Xylenes of alcohols were used for dilution and for controlling solution viscosity at 10–100 cP. The films on YSZ and LAO were deposited by spin coating at 3000–3500 rpm and were dried at 200–250 °C for several minutes. This process was repeated to build up the desired film thickness (0.3–0.6 μm). The films were heated at 800–920 °C under controlled atmosphere and further O_2 annealed at 400 °C for 24 h. The substrates used in this experiment were commercial YSZ and LAO single crystals with the (0 0 1) orientation. Both YSZ and LAO single crystals had dimensions of $12 \times 12 \times 1$ mm^3 and were purchased from MTI Company. One side of the single crystal was polished as-purchased.

A Philip X-ray diffractometer with CuK_α radiation was used to carry out the texture investigations. The X-ray wavelength was 1.54 Å with a beam size of 3 mm. Scanning electron microscopy (SEM) experiments were performed on a Hitachi 2000. Some specimens were also examined by SEM in a JEOL JSM 5400 microscope that was operated at 10 kV. No conductive coating was applied. The high-resolution transmission electron microscopy (HRTEM) experiments were performed on a JEOL JEM 4000EX TEM. Transport resistivity and current density measurements were carried out down to liquid-helium temperature at zero magnetic field using a standard four-probe method.

3. Results and discussion

The YBCO sol–gel solutions were deposited on both YSZ and LAO substrates via spin coating. Using the heat-treatment procedures described in the experimental details, we obtained well-textured YBCO thin films on both of these substrates. The X-ray diffraction (XRD) analysis of the film on YSZ and LAO are shown in Fig. 1. As can be seen in Fig. 1a, all of the (0 0 l) peaks of the YBCO on YSZ indicate a well-textured, *c*-axis oriented grain structure. A similar XRD pattern can be seen in Fig. 1b for the YBCO film on LAO. These are quite typical XRD patterns observed from most of sol–gel films on YSZ and LAO in our experiments. In Fig. 2, SEM image shows, from a top view, that the YBCO film appears to have a multi-grain

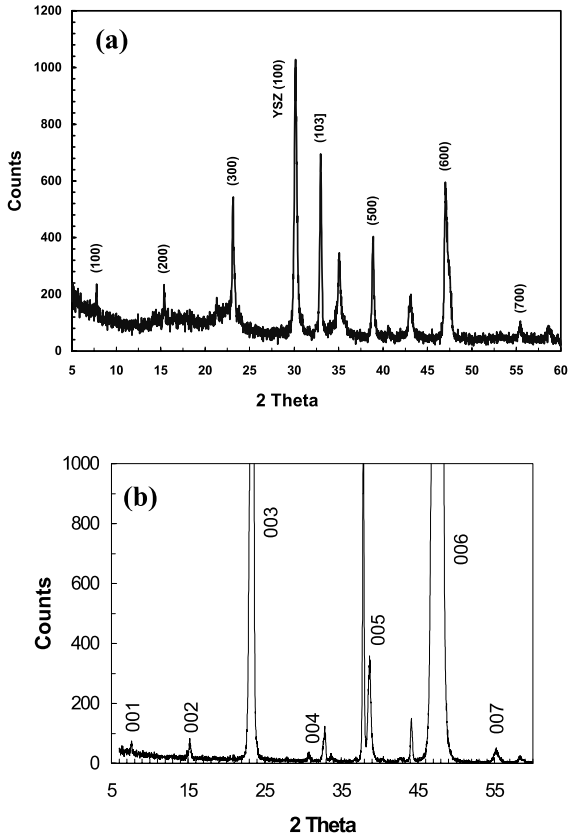

Fig. 1. XRD spectra of YBCO films on (a) YSZ and (b) on LAO.

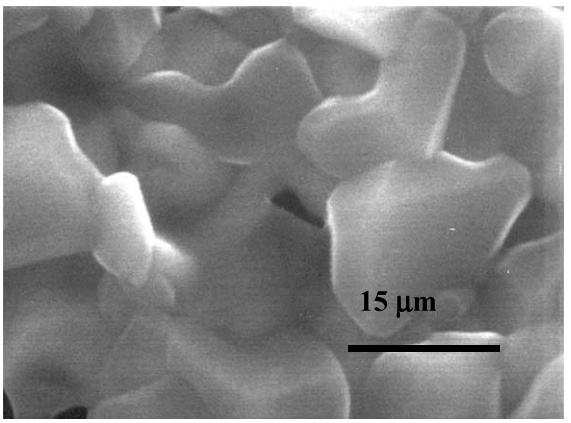

Fig. 2. SEM photo micrograph, showing the top surface of YBCO film on YSZ.

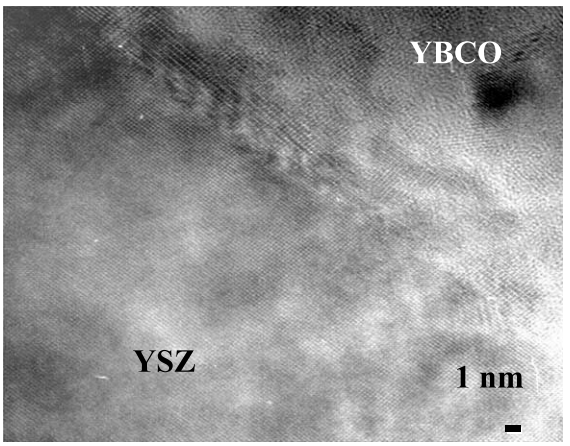

Fig. 3. HRTEM image showing the interface lattice structure of YBCO on YSZ.

structure, but is quite dense with sharp irregular edges rather than the typical platelets.

The textured structures in these sol–gel films were confirmed by HRTEM. Fig. 3 shows the interface lattice structure of the YBCO film on YSZ. In this figure, the YBCO film is on the top, right, with coherent lattice with the YSZ substrate, indicating that the growth of YBCO film is clearly epitaxial at the interface. In Fig. 4, we show the interface and diffraction patterns of sol–gel YBCO film on YSZ. Fig. 4a is similar to Fig. 3, however, shown here are its diffraction patterns (Fig. 4b–d). Fig. 4b is the Fourier transformation of image 4a showing two sets of diffraction patterns. The circles are for visual aid and indicate the size of mask for the filtered images in Fig. 4c and d. The thicklined circles are of YBCO and thin lines are of YSZ. Fig. 4c is a filtered image using the indicated masks. The arrows indicate the lattice mismatching at about every seven lattices (1 1 0) of YSZ. Fig. 4d is another filtered image using indicated masks. The (0 0 3) plane of YBCO is tilted about 5° from the (0 0 1) plane of YSZ (Fig. 4b–d).

Fig. 5 shows an SEM image of the YBCO film on LAO, with a smooth and dense microstructure. The textured grains are also confirmed by rocking-curve results shown in Fig. 6. The rocking curves shown in Fig. 6 are clear indications that the YBCO film has a well-aligned grain orientation. Fig. 6a shows the rocking curve of the LAO

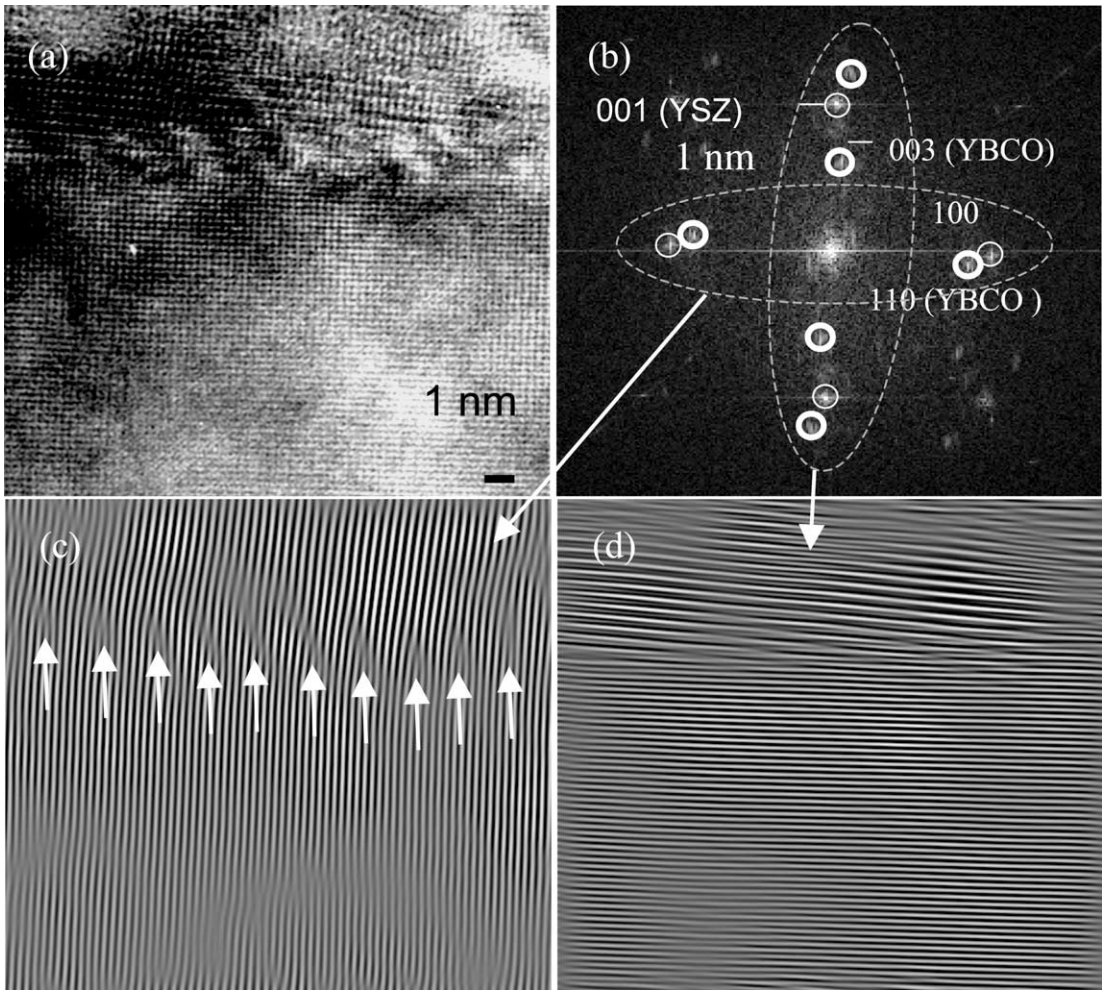

Fig. 4. HRTEM image showing the interface structure and diffraction pattern of YBCO film on YSZ: (a) interface lattice structure; (b) the Fourier transformation of the image; (c) the filtered image using the indicated masks, and (d) additional filtered image using the indicated masks.

substrate with the (0 0 1) orientation. In Fig. 6, the (0 0 5) peak of YBCO rocking curve exhibits a full width at half maximum of 0.18° indicating an excellent *c*-axis orientation of the grains. The epitaxial nature of the YBCO on LAO can be clearly seen from the HRTEM interface image shown in Fig. 7. Similar to Fig. 3, the lattice structures of YBCO and LAO form a coherent interface as shown in Fig. 7.

Epitaxial growth of YBCO thin films on both YSZ and LAO are expected since the substrates are single crystalline. With controlled deposition, the YBCO phase crystallizes according to the orientation of the substrate. However, in previous reports [6–16], a $BaZrO_3$ (BZO) buffer layer often forms at the interface in fluorine-based sol–gel films. In contrast, in well-controlled temperature range below 810 °C, we did not observe any BZO layer in our sol–gel films on both YSZ and LAO. It should be noted that, however, as the temperature was increased to above 810 °C, BZO layer did form in the non-fluorine-based sol–gel films. Fig. 8 shows the bright-field TEM image of YBCO/YSZ interface. As shown in this figure a BZO buffer

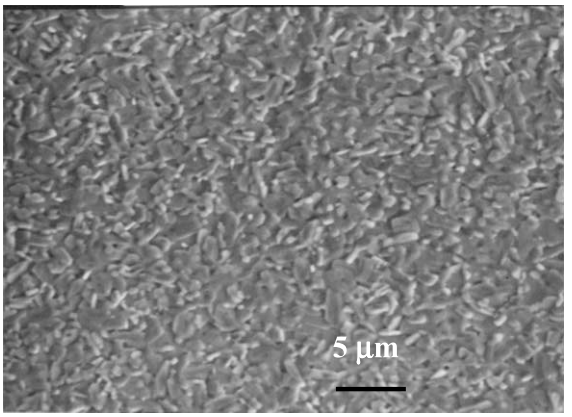

Fig. 5. SEM photo micrograph showing the top surface of YBCO film on LAO.

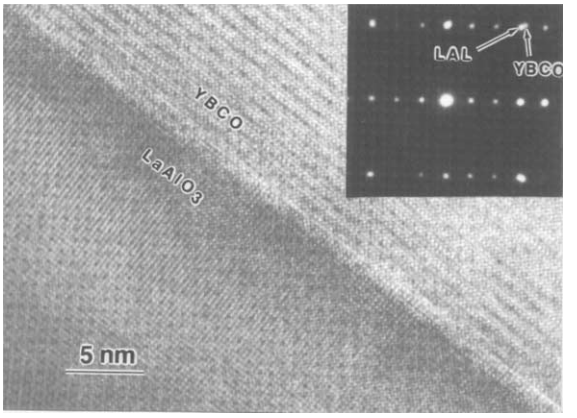

Fig. 7. HRTEM image showing the interface lattice structure of YBCO on LAO.

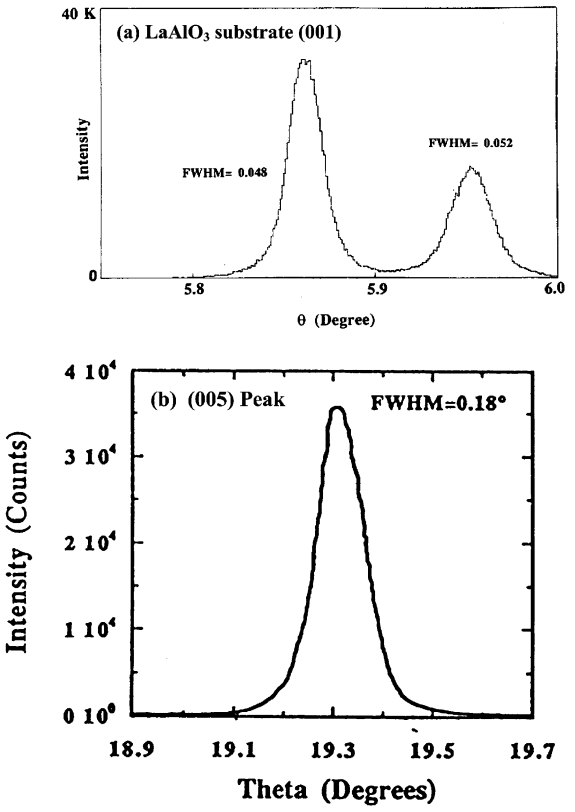

Fig. 6. XRD rocking curves of (a) LAO substrate (0 0 1) and (b) YBCO film (0 0 5) on LAO.

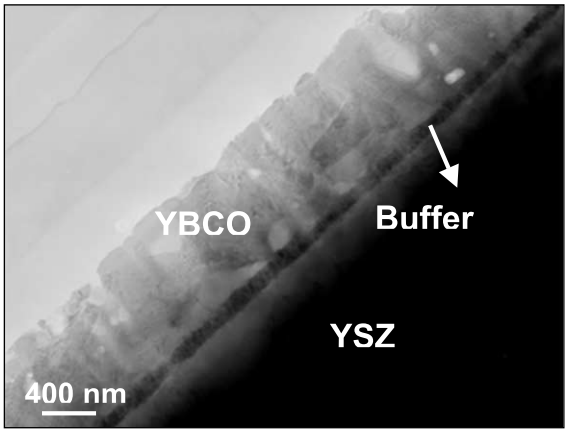

Fig. 8. Bright-field TEM image of YBCO/YSZ interface showing a BZO buffer layer at the interface.

layer exists at the interface. The EDS analysis of the YBCO film, the BZO layer, and the LAO substrate is shown in Fig. 9 confirming the identity of the BZO buffer layer.

The oxygenated films on all substrates were characterized by four-probe measurement. The results are shown in Figs. 10 and 11. Both films on YSZ and LAO exhibit sharp T_c values near 90 K. The effect of heat-treatment temperature on transport T_c is also shown in Fig. 11. From this figure, we can see that the superconducting transitions are sensitively affected by the heat-treatment temperature. At 790 °C, the normal state exhibits a semiconducting behavior that is improved by increasing the temperature to 800 °C.

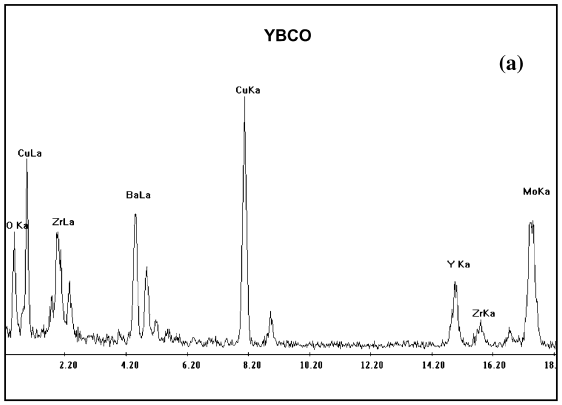

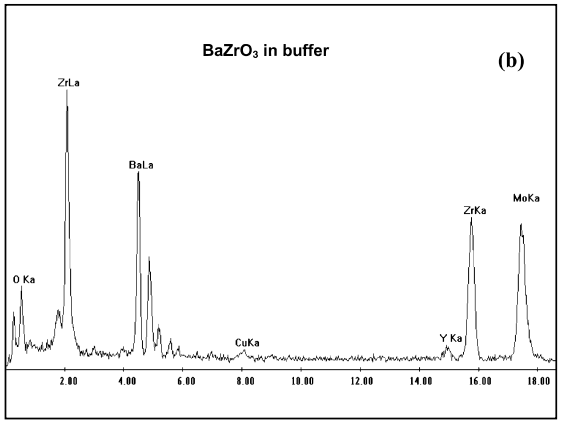

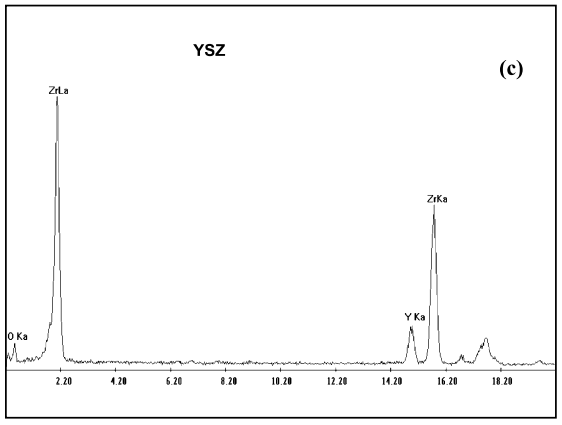

Fig. 9. The EDS analysis of the interface area in the YBCO/YSZ film: (a) the YBCO film; (b) BZO buffer layer; and (c) the YSZ buffer.

However, further increasing the temperature to 810 °C causes the normal resistivity to increase significantly. Therefore the optimum heat-treatment

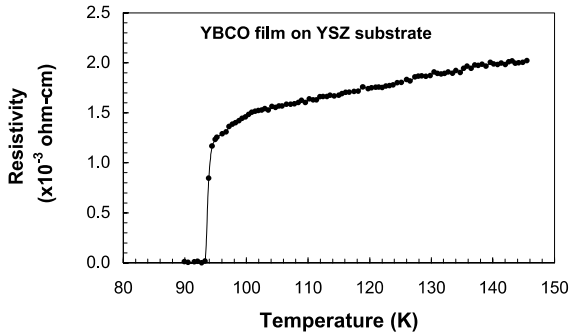

Fig. 10. Resistivity versus temperature for the YBCO film on YSZ single-domain substrate.

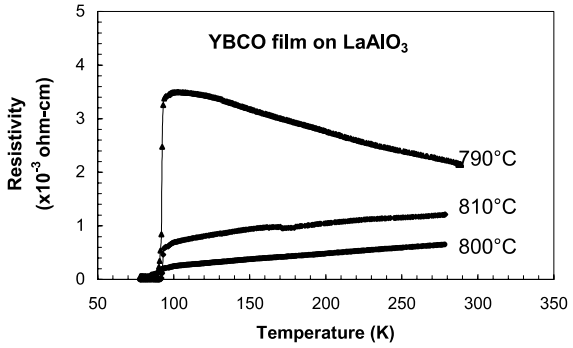

Fig. 11. Resistivity versus temperature for the YBCO films on LAO at heat-treatment temperatures indicated.

temperature is only within a narrow window of <20 °C. As noted above, BZO buffer forms above 810 °C. Therefore, the optimization of processing parameters has been conducted below this temperature.

Preliminary measurements on the transport critical current density were performed using the four-probe method using a 10^{-6} V/cm voltage criterion. The sample dimensions were $15 \times 3 \times 0.0004$ mm^3. As shown in Fig. 12, the transport J_c has been determined as a function of temperature in zero field for YBCO on LAO. At 77 K, the transport J_c of YBCO on LAO has reached a value above 10^5 A/cm^2 at 77 K and zero magnetic field. However, this value is expected to be improved as the processing parameters are optimized.

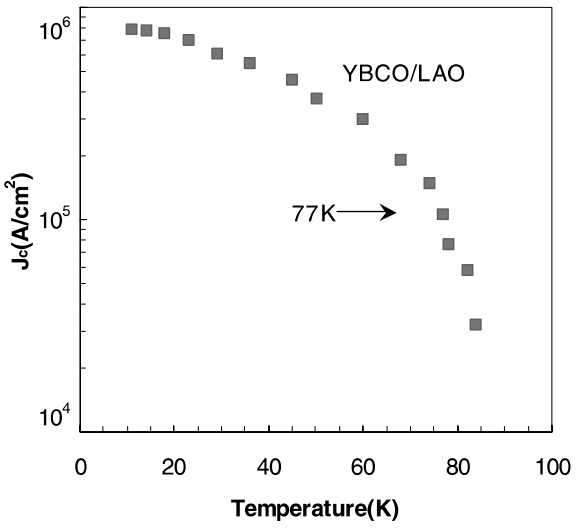

Fig. 12. Transport J_c versus temperature for the YBCO film on LAO at zero magnetic field.

4. Summary

In summary, we have deposited YBCO thin films on YSZ and LAO substrates using a fluorine-free sol–gel approach. Both XRD and HRTEM results have shown that the sol–gel YBCO films on both YSZ and LAO exhibit the *c*-axis grain orientation with coherent epitaxial interface structures. Above 810 °C, a BZO buffer layer forms at the interface in the YBCO film on LAO. All films exhibit sharp T_cs near 90 K. A transport J_c above 10^5 A/cm^2 has been obtained in the YBCO film on LAO.

Acknowledgements

We would like to thank John Sundeen and Steve Herbert for their help in sol–gel synthesis and superconducting-property evaluation. The TEM analyses were conducted at the Electron Microbeam Analysis Laboratory at the University of Michigan, Ann Arbor, Michigan. Work at Argonne was supported by the US Department of Energy (DOE), Energy Efficiency and Renewable Technology, as part of a DOE program to develop electric power technology, under contract W-31-109-Eng-38.

References

[1] A. Goyal et al., Appl. Supercond. 4 (1996) 403–427.
[2] M. Paranthaman et al., Proc. 9th Int. Symp. Supercond., Sapporo, Hokkaido, Japan, 21–24 October 1996.
[3] X.D. Wu et al., Appl. Phys. Lett. 65 (1994) 1961.
[4] D. Shi, D. Qu, X. Wen, B.A. Tent, M. Tomsic, J. Supercond. 11 (1998) 575.
[5] D. Shi, Y. Xu, S.X. Wang, L.M. Wang, S.M. McClellan, Physica C 353 (2001) 258–264.
[6] M.E. Gross, M. Hong, S.H. Liou, P.K. Gallagher, J. Kwo, Appl. Phys. Lett. 52 (1988) 160–162.
[7] M.L. Kullberg, M.T. Lanagan, W. Wu, R.B. Poeppel, Supercond. Sci. Technol. 4 (1989) 337–342.
[8] Y.L. Chen, J.V. Mantese, A.H. Hamdi, A.L. Mecheli, J. Mater. Res. 4 (1989) 1065–1071.
[9] K. Yamagiwa, H. Hiei, Y. Takahashi, S.B. Kim, K. Matsumoto, H. Ikuta, U. Mizutani, I. Hirabayashi, Physica C 334 (2000) 301–305.
[10] A. Gupta, R. Jagannathan, E.I. Cooper, E.A. Geiss, J.I. Landman, B.W. Hussey, Appl. Phys. Lett. 52 (1988) 2077–2079.
[11] P.C. McIntyre, M.J. Cima, J.A. Smith Jr., R.B. Hallock, M.P. Siegal, J.M. Phillips, J. Appl. Phys. 71 (1992) 1868–1877.
[12] P.C. McIntyre, M.J. Cima, A. Roshko, J. Appl. Phys. 77 (1995) 5263–5272.
[13] S. Sathyamurthy, K. Salama, Physica C 329 (2000) 58–68.
[14] A. Malozemoff, S. Annavarapu, L. Fritzmeier, Q. Li, V. Prunier, M. Rupich, C. Thieme, W. Zhang, A. Goyal, M. Paranthaman, D.F. Lee, Supercond. Sci. Technol. 13 (2000) 473–476.
[15] Y. Jee, B. Ma, V.A. Maroni, M. Li, B.L. Fisher, U. Balachandran, Supercond. Sci. Technol., in press.
[16] D. Shi, Y. Xu, S. McClellan, R. Buchanan, Physics C 354 (2001) 71–76.